Giant Density of States Enhancement Driven by a Zero-Mode Landau Level in Semimetallic Black Phosphorus under Pressure

Takuto Fujii,[1,*] Yusuke Nakai,[1] Michihiro Hirata,[2,†] Yasumasa Hasegawa,[1] Yuichi Akahama,[1] Koichi Ueda,[1] and Takeshi Mito[1,‡]

[1]*Department of Material Science, Graduate School of Science, University of Hyogo, 3-2-1 Kouto, Kamigori-cho, Ako-gun, Hyogo 678-1297, Japan*

[2]*Institute for Materials Research, Tohoku University, Sendai 980-8577, Japan*

(Received 7 July 2022; accepted 26 January 2023; published 17 February 2023)

Dirac fermion systems form a unique Landau level at the Fermi level—the so-called zero mode—whose observation itself will provide strong evidence of the presence of Dirac dispersions. Here, we report the study of semimetallic black phosphorus under pressure by ^{31}P-nuclear magnetic resonance measurements in a wide range of magnetic field up to 24.0 T. We have found a field-induced giant enhancement of $1/T_1T$, where $1/T_1$ is the nuclear spin lattice relaxation rate: $1/T_1T$ at 24.0 T reaches more than 20 times larger than that at 2.0 T. The increase in $1/T_1T$ above 6.5 T is approximately proportional to the squared field, implying a linear relationship between the density of states and the field. We also found that, while $1/T_1T$ at a constant field is independent of temperature in the low-temperature region, it steeply increases with temperature above 100 K. All these phenomena are well explained by considering the effect of Landau quantization on three-dimensional Dirac fermions. The present study demonstrates that $1/T_1$ is an excellent quantity to probe the zero-mode Landau level and to identify the dimensionality of the Dirac fermion system.

DOI: 10.1103/PhysRevLett.130.076401

The fascinating physical properties of substances simply made up of a single element can trigger progress of advanced solid state physics. Graphene, in which the existence of the massless Dirac fermions was first discovered [1], is a typical example, and it opened the way to a new research field of massless fermions incorporating relativistic effects. Black phosphorus (BP), one of the allotropes of phosphorus, is another single-element substance that has recently attracted much attention. BP with a puckered graphenelike honeycomb layered structure is a semiconductor, and this fact is in contrast to the gapless and metallic properties of graphene and graphite, respectively. The moderate energy gap size of BP, which can be controlled by the number of phosphorene layers (0.3 eV for the bulk to 2 eV for the monolayer) [2–6], and excellent transport properties, including high carrier mobility and strongly anisotropic conduction, promise its potential for applications to high-performance devices (see, e.g., Ref. [7] and references therein).

In addition, BP is one of a few candidate materials in which the appearance of 3D Dirac dispersions is tuned by the application of pressure [8,9]. Therefore, the issue of interest in this study is the extension of the two-dimensional (2D) Dirac dispersion, found in graphene, to three-dimensional (3D) systems. BP undergoes a transition from a normal semiconducting phase to a semimetallic phase at a transition pressure of 1.2–1.5 GPa, as evidenced by a gap estimation from an optical absorption measurement [10] and the observation of Shubnikov–de Haas oscillation [11–13]. This transition is also viewed as a topological change in the Fermi surface [11–14]. Above this critical pressure, BP is theoretically predicted to be a 3D Dirac semimetal with Dirac cones [8] or a node line [9,15]. Experimentally, on the other hand, although the emergence of a nontrivial Berry phase has been suggested as evidence for Dirac-like dispersion by transport experiments [11,13], there are actually a few experimental techniques to investigate the band structure under pressure, albeit in the easy-to-reach pressure region for BP. Thus, the presence of Dirac dispersions in BP has not been confirmed.

Worth noting is that the Dirac fermion systems form unique Landau levels in a magnetic field, depending on their dimensionality: In both 2D and 3D systems, a Landau level at the Fermi energy ε_F appears, which is called the zero mode [16–18], but they show a different magnetic field response, as described later. In this Letter, we have focused on observing the field dependence of the density of states (DOS) at the zero mode. The observation of the zero mode is itself strong evidence of the existence of Dirac dispersions, and its magnetic field dependence provides crucial information on dimensionality.

For nonmagnetic materials, the nuclear spin lattice relaxation rate $1/T_1$ measured by the nuclear magnetic resonance (NMR) technique reflects the DOS following Eq. (1) [19]:

$$\frac{1}{T_1} = \pi\gamma^2\hbar A_{\mathrm{hf}}^2 \int_{-\infty}^{\infty} D(\varepsilon)^2 f(\varepsilon-\mu)\{1-f(\varepsilon-\mu)\}d\varepsilon, \quad (1)$$

where γ is the nuclear gyromagnetic ratio, A_{hf} is the hyperfine coupling constant, $D(\varepsilon)$ is the energy dependence of the DOS, μ is the chemical potential, and $f(\varepsilon-\mu)$ is the Fermi-Dirac distribution function. The NMR is well known as a low-energy probe, and, therefore, when measuring it on the Dirac fermion systems at low temperatures and high magnetic fields, the T_1 relaxation should be dominated by the DOS at the zero mode. To extract the zero-mode component in the high-pressure semimetallic phase of BP, we have carried out the T_1 measurements in a wide range of magnetic field from 2.0 to 24.0 T and a temperature range of 4.2–300 K.

A polycrystalline sample of BP was prepared by a high-pressure synthesis technique [20]. The high-pressure measurements of ^{31}P-NMR were carried out using a self-clamped BeCu/NiCrAl piston-cylinder cell. The BP sample, an NMR coil, a manganin wire gauge, and a tin manometer were placed inside a Teflon capsule filled with silicon-based organic liquid as a pressure-transmitting liquid. The pressure was loaded by monitoring the manganin gauge, and the clamped pressure was determined by measuring the superconducting transition temperature of the tin. The estimated pressure is 1.63 GPa, just above the semiconductor-semimetal transition pressure. ^{31}P-NMR spectra and T_1 relaxation curves were acquired by measuring the intensity of free induction decay signal using a phase-coherent pulsed spectrometer (Thamway Co., Ltd., Japan). The wide range of magnetic field measurements are realized by using 8 and 15 T superconducting magnets (SMs) at University of Hyogo ($2.0 < B < 13.0$ T) and a 25 T cryogen-free SM (25T-CSM) ($13.0 < B < 24.0$ T) at Tohoku University. For details on the stability of these SMs to measure the long T_1 of BP, see Supplemental Material [21].

Figure 1 shows the representative comparison of T_1 relaxation curves measured at different applied fields. The value of T_1 is determined by fitting the relaxation curves to a single exponential function expected for ^{31}P with a nuclear spin $I = 1/2$. Note that, over the entire temperature and field range, the T_1 recovery curves consist of a single component within experimental accuracy (in addition to Fig. 1, see Fig. S3 in Supplemental Material [21]). We found that T_1 at 13.0 T is approximately one-third of that at 6.5 T (see Fig. 1), and the obvious difference in the slope of the two curves indicates the unambiguous effect of field on T_1. More detailed field dependence over a wide range of fields from 2.0 to 24.0 T and at a fixed temperature of 4.2 K is shown in Fig. 2. $1/T_1T$ reveals a noticeable increase with increasing field, in particular, above 10.0 T: The increase at 24.0 T reaches more than 20 times compared to the lowest field (2.0 T). Field-induced variations in T_1 are seen in magnetic materials, because spin fluctuations are suppressed by the strong magnetic field. The effects of strong field are also expected in low carrier density systems and narrow-gap semiconductors: When applying strong fields beyond the quantum limit, all electrons occupying the lowest Landau level are fully spin polarized and the electron spin can no longer flip [23]. In both cases, $1/T_1T$ is reduced by the magnetic field; therefore, the observed anomalous *increase* in $1/T_1T$ with field is unprecedented for conventional materials as far as the authors know.

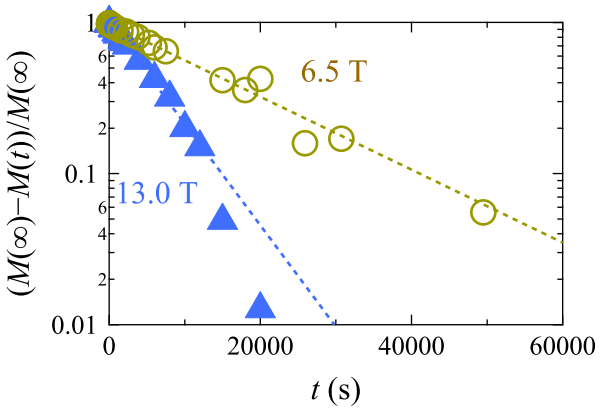

FIG. 1. T_1 recovery curves measured at 4.2 K and different external fields of 6.5 and 13.0 T. $[M(\infty)-M(t)]/M(\infty)$ is plotted as a function of t, where t is a delay time after the saturation pulses and $M(t)$ is the nuclear magnetization at t. The dotted lines are fits to a single exponential function $\exp(-t/T_1)$.

In the following analyses, we incorporate the Landau quantization within 2D and 3D Dirac fermion models,

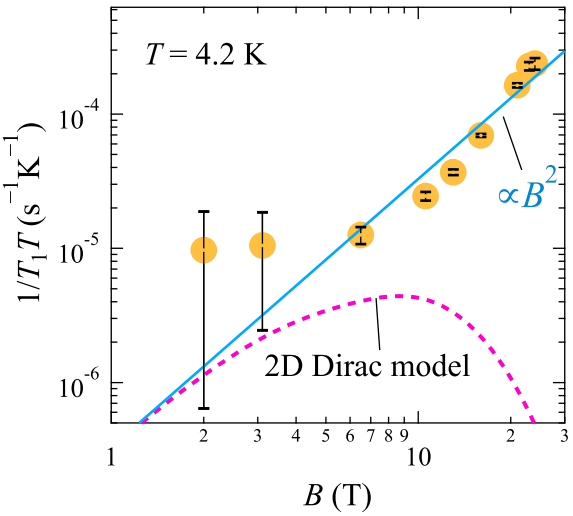

FIG. 2. Field dependence of $1/T_1T$ (open circles) measured at 4.2 K. The red dotted line shows the field dependence expected for the 2D Dirac fermion system, where we assumed the model illustrated in the inset in Fig. 3. The blue solid line represents the least-squares fit of the B^2 function to the data above 6.5 T, where the B^2 law is the field dependence expected for the 3D Dirac fermion system. See the text for details.

which is essential to the effects of field on the DOS in the Dirac fermion systems at low temperatures. When a magnetic field B is applied to a 2D Dirac fermion system, the DOS separates into energy-discrete levels with the Landau level index n, and a zero-mode ($n = 0$) DOS appears at the energy of the Dirac point, ε_D [17]. As the magnitude of the zero-mode DOS increases in proportion to B, $1/T_1T$ will follow an approximately B^2 increase using Eq. (1). However, at the same time, one needs to consider the spin splitting of the zero mode due to the Zeeman effect, as shown in the inset in Fig. 3. Then, the magnitude of the DOS at $\varepsilon = \varepsilon_D$ will undergo a maximum as the field increases, followed by a monotonic decrease. Indeed, the quasi-2D Dirac material α-$(BEDT\text{-}TTF)_2I_3$ exhibits the maximum in the electronic specific heat coefficient, as evidenced by a specific heat measurement [24].

Although the magnetic field for the maximum may depend on the species of 2D Dirac material, it is, in principle, determined by the combination of the following two factors: the field dependence of the magnitude of the zero-mode DOS and its spin splitting. For the rough estimation of the field for the maximum, we assume a Gaussian-shaped zero-mode DOS with a width thermally broadened as k_BT and its spin splitting of $g\mu_BB$, where k_B is the Boltzmann constant, $g \approx 2$ [25] is the Landé g factor, and μ_B is the Bohr magneton. The calculation of the field dependence of $1/T_1T$ at $T = 4.2$ K gives a maximum around 8 T, as indicated by the red dotted line in Fig. 2. The maximum field of this experiment—24.0 T—would be large enough to observe a downward deviation from the B^2 dependence; however, there is no sign of that happening at all in the present data. Thus, the 2D Dirac fermion model is incompatible with the present results.

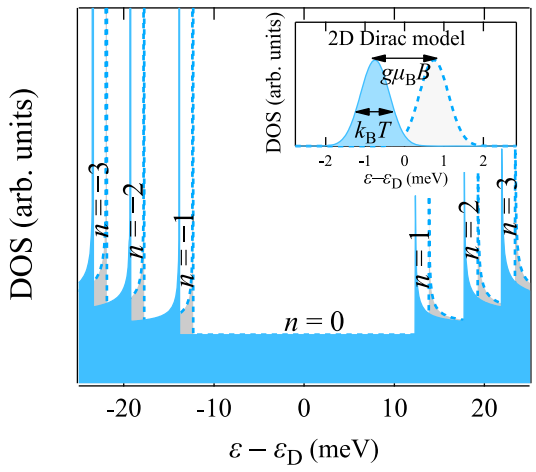

FIG. 3. Energy dependence of the DOS of the 3D Dirac fermion system, which is calculated based on Ref. [26] and Eq. (2) assuming $B = 13.0$ T and $v_F = 1 \times 10^5$ m/s. Inset: the zero-mode DOS of the 2D Dirac fermion system. For the Zeeman splitting, we assume $B = 13.0$ T. The solid and dashed lines are the DOS for up and down spins, respectively.

In contrast, different field dependence of $1/T_1T$ is expected for the 3D Dirac fermion systems. The effect of the Landau quantization on a simple 3D Dirac fermion system leads to the following energy dependence of the DOS [27,28]:

$$D_0(E) = \frac{eB}{4\pi^2\hbar c v_F}\left(1 + 2\sum_{n=1}^{\lfloor E^2/2v_F^2 e\hbar B\rfloor}\frac{|E|}{\sqrt{E^2 - 2v_F^2 e\hbar nB}}\right), \tag{2}$$

where c is a velocity of light, $\lfloor x \rfloor$ is the integer part of x, v_F is the Fermi velocity, and $E = \varepsilon - \varepsilon_D$. If the Zeeman splitting of the Landau quantization is also taken into account, $D_0(E)$ in Eq. (2) is modified into $D(E)$ in Ref. [26]. $D(E)$ acquires a sawtooth form with divergences at $E_n \pm g\mu_BB/2$, where $n = \pm1, \pm2, \pm3\ldots$ and

$$E_n(B) = \begin{cases} -v_F\sqrt{2e\hbar|n|B} & (n < 0) \\ v_F\sqrt{2e\hbar|n|B} & (n > 0), \end{cases} \tag{3}$$

and an energy-independent zero mode ($n = 0$) that appears between the divergences for $n = \pm1$, as illustrated in Fig. 3. For $n = 0$, the magnitude of the zero-mode DOS is in proportion to B, as Eq. (4) indicates:

$$D(E) = \frac{eB}{2\pi^2\hbar c v_F}(n = 0). \tag{4}$$

Unlike the zero-mode DOS in the 2D system, the spin splitting effect is effectively negligible because of the energy-independent shape of the DOS around $E = 0$. Therefore, if B is large enough—namely, E_1 is much larger than the thermal excitation energy—B^2 dependence is expected in $1/T_1T$ according to Eq. (1). As indicated by the blue solid line in Fig. 2, the result above 6.5 T is much more in accordance with this 3D model than with the 2D model.

Below 6.5 T, $1/T_1T$ exhibits remarkable deviation from B^2 dependence, and we here briefly comment on this feature. As the field decreases, $E_{n\geq1}$ approaches $E = 0$, and the enhanced DOS at $E_{n\geq1}$ begins to contribute to the T_1 relaxation. Since this additional effect will weaken the field dependence of $1/T_1T$ ($\propto B^2$) originating from the zero mode, the much less field dependence observed below 6 T may result from such a scheme. However, quantitative simulations in the low-field region are difficult, for example, because the features of the original band structure at zero field remain strong and/or quantum oscillations may appear as observed in the magnetoresistance [11–13].

The validity of the 3D model can also be examined from the temperature dependence of $1/T_1T$ measured at different magnetic fields. Figure 4 shows the comparison of $1/T_1T$ measured at 6.5 and 13.0 T. Above 100 K, the two series of

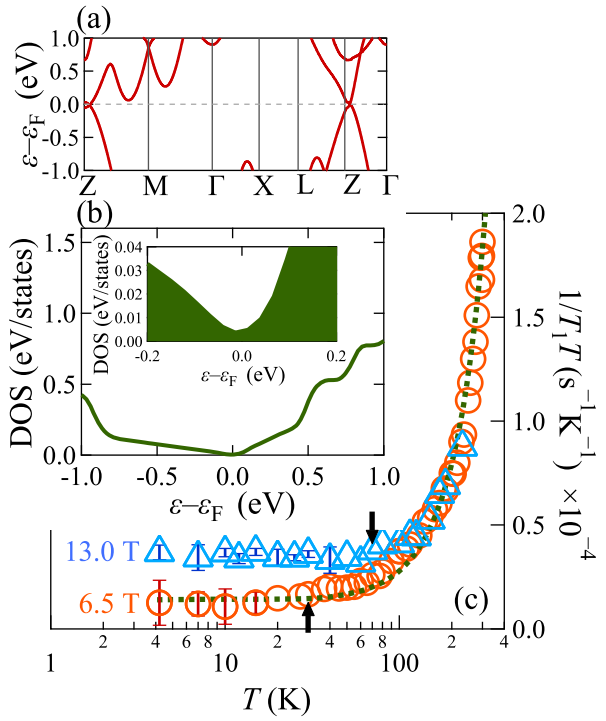

FIG. 4. (a) Band structure near ε_F calculated by the LDA with structural parameters at 1.55 GPa [29,30]. (b) Energy dependence of the total DOS based on the result shown in (a). The inset shows an expanded view near ε_F. (c) Temperature dependence of $1/T_1T$ at 6.5 (open circles) and 13.0 T (solid triangles) and at 1.63 GPa. The dotted line is the result of computing Eq. (1) using the DOS shown in (b). The arrows denote T^* at 6.5 and 13.0 T. Error bars sufficiently smaller than the size of symbols are not shown.

data coincide, suggesting that thermal fluctuations surpass the field effect on $1/T_1T$ observed at low temperatures (see Fig. 2). The temperature dependence above 100 K is well reproduced by the calculation of Eq. (1) as indicated by the dotted line, where we used the DOS [see Fig. 4(b)] obtained from the local density approximation (LDA) calculation plus the modified Becke-Johnson exchange potential [see Fig. 4(a)]. Here, we adopted the recently reported crystallographic parameters at 1.55 GPa [29,30]. As shown in Fig. 4(a), the present LDA calculation, as well as the previous reports [8,9], predicts the existence of 3D Dirac dispersions around the Z point of the Brillouin zone. This prediction is well supported by the above-mentioned consistency between the experiment and the calculation of $1/T_1T$ above 100 K in the semimetallic state, together with similar consistency in the semiconducting state below 1 GPa [31].

As the temperature decreases below 200 K, the temperature gradient of $1/T_1T$ gradually decreases at both 6.5 and 13.0 T, followed by constant behavior against the temperature. Such temperature-independent behavior is also derived from the simulation using Eq. (1) based on the LDA calculation, as the dotted line shows in Fig. 4(c). In this case, it is interpreted that the temperature dependence is mainly attributed to the tiny DOS at ε_F, as indicated in the inset in Fig. 4(b), where the DOS near ε_F is expanded. However, in this temperature region below about 100 K, the effect of magnetic field on $1/T_1T$ becomes distinct: $1/T_1T$ at 13.0 T is enhanced compared to that at 6.5 T. Moreover, the temperature below which $1/T_1T$ is temperature independent, defined as $T^*(B)$, depends strongly on B, i.e., $T^*(13.0\mathrm{T}) = 75 \pm 5$ K and $T^*(6.5\mathrm{T}) = 30 \pm 5$ K as indicated by the arrows in Fig. 4(c). These cannot be explained by the present LDA calculation, because the effect of field is not taken into account in it.

Therefore, we again consider the effect of the Landau quantization to understand these phenomena driven by field. Based on the Landau level scheme for the 3D Dirac fermion system, the flat zero-mode DOS (see Fig. 3) will induce $1/T_1T = \text{const}$ behavior in the low-temperature region, and the field dependence of $1/T_1T$ is accounted for in the regime of Eq. (4) as described above. In order to explain the upward deviation of $1/T_1T$ from the constant above T^* and the field-dependent $T^*(B)$, the contribution of the highly enhanced DOS at $E_n(B)$ with $n = 1$ or -1 is essential, where $n = 1$ if $\mu > \varepsilon_D$ and $n = -1$ if $\mu < \varepsilon_D$. We also take into account the field dependence of μ as follows: From the inversely proportional relationship between n and the magnetic field at which the Shubnikov–de Haas oscillation in the longitudinal resistance exhibits a dip, we obtain $B|n| \approx 4.5$ T [12]. Here, the Landau level index for $n < 0$ is also included. Then we assume $\mu(4.5\,\mathrm{T}) = E_\alpha(4.5\,\mathrm{T})$, where $\alpha = 1$ if $\mu > \varepsilon_D$ and $\alpha = -1$ if $\mu < \varepsilon_D$. For $B > 4.5$ T, since $E_{-1} < \mu(B) < E_1$ and $D(E) \propto B$ [see Eq. (3)], $\mu(B)$ is given as $\mu(B) = E_\alpha(4.5\ \mathrm{T}) \times (4.5/B)$. Moreover, the assumption that $T^*(B) \propto |E_\alpha(B) - \mu(B)|$ and the relationship that $E_{\pm1}(B) = E_{\pm1}(4.5) \times \sqrt{B/4.5}$ from Eq. (3) yield $T^*(13.0\ \mathrm{T})/T^*(6.5\ \mathrm{T}) \sim 2.66$, where Zeeman splitting is also considered. This estimation is in excellent agreement with the experimental result of 2.7 ± 0.5, which provides a plausible explanation of the peculiar field dependence of T^*, although whether μ is greater or less than ε_D, and, hence, the sign of α, cannot be determined only by this study.

Thus, the present study successfully detects the zero-mode DOS, which provides direct evidence that BP is a 3D Dirac semimetal. However, looking at the details of the field dependence of $1/T_1T$ shown in Fig. 2, the experimentally obtained field dependence above 10 T seems slightly steeper than the B^2 law indicated by the present model. This small discrepancy may be because our model does not reflect the real band structure of BP. For example, the existence of a node line rather than simple Dirac points is theoretically predicted near E_F [9,13]. Moreover, since a polycrystalline sample was used in this study, it is possible that the value of $1/T_1T$, which can depend on the direction of the applied field reflecting anisotropy in the k space, is rounded in some way. It is, therefore, expected that

measurements using a single crystalline sample will allow us to identify the effect of the Landau quantization on a more realistic band structure. Such measurements are currently in progress, and it has revealed that the anisotropy of T_1 is small at ambient pressure [32].

In summary, we observed an enormous field-induced increase of $1/T_1T$ at 1.63 GPa, just above the semiconductor-semimetal transition pressure of BP: $1/T_1T$ above 6.5 T increases with the approximately B^2 law, implying that the DOS changes in proportion to B, and its value at 24.0 T reaches 20 times larger than that at 2.0 T. $1/T_1T$ measured at a constant field shows temperature-independent behavior in the low-temperature region, whereas it steeply increases with increasing temperature above T^* that strongly depends on the field. All these phenomena are well explained by considering the Landau quantization effect within a 3D Dirac fermion model. The present study shows that the observation of the zero-mode Landau level by the $1/T_1$ measurement, capable of high-pressure measurements as well, is highly useful for identifying the Dirac dispersion.

We acknowledge T. Nomura for his assistance in conducting the band calculations. This work was performed under the GIMRT Program of the Institute for Materials Research, Tohoku University (Proposal No. 19H0032), and supported by JSPS KAKENHI (Grants No. 18H04331, No. 15H05883, No. 18K03545, No. 21K03475, and No. 21K03450).

*Present address: Max Planck Institute for Chemical Physics of Solids, 01187 Dresden, Germany.
†Present address: MPA-Q, Los Alamos National Laboratory, Los Alamos, 87545 New Mexico, USA.
‡mito@sci.u-hyogo.ac.jp

[1] K. S. Novoselov, A. K. Geim, S. V. Morozov, D. Jiang, M. I. Katsnelson, I. Grigorieva, S. Dubonos, and A. Firsov, Nature (London) **438**, 197 (2005).
[2] V. Tran, R. Soklaski, Y. Liang, and L. Yang, Phys. Rev. B **89**, 235319 (2014).
[3] H. Liu, A. T. Neal, Z. Zhu, Z. Luo, X. Xu, D. Tománek, and P. D. Ye, ACS Nano **8**, 4033 (2014).
[4] L. Liang, J. Wang, W. Lin, B. G. Sumpter, V. Meunier, and M. Pan, Nano Lett. **14**, 6400 (2014).
[5] X. Wang, A. M. Jones, K. L. Seyler, V. Tran, Y. Jia, H. Zhao, H. Wang, L. Yang, X. Xu, and F. Xia, Nat. Nanotechnol. **10**, 517 (2015).
[6] J. Yang, R. Xu, J. Pei, Y. W. Myint, F. Wang, Z. Wang, S. Zhang, Z. Yu, and Y. Lu, Sci. Appl. **4**, e312 (2015).
[7] X. Mu, J. Wang, and M. Sun, Mater. Today Phys. **8**, 92 (2019).
[8] P. L. Gong, D. Y. Liu, K. S. Yang, Z. J. Xiang, X. H. Chen, Z. Zeng, S. Q. Shen, and L. J. Zou, Phys. Rev. B **93**, 195434 (2016).
[9] J. Zhao, R. Yu, H. Weng, and Z. Fang, Phys. Rev. B **94**, 195104 (2016).
[10] Y. Akahama and H. Kawamura, Phys. Stat. Solids (b) **223**, 349 (2001).
[11] Z. J. Xiang, G. J. Ye, C. Shang, B. Lei, N. Z. Wang, K. S. Yang, D. Y. Liu, F. B. Meng, X. G. Luo, and L. J. Zou, Phys. Rev. Lett. **115**, 186403 (2015).
[12] K. Akiba, A. Miyake, Y. Akahama, K. Matsubayashi, Y. Uwatoko, H. Arai, Y. Fuseya, and M. Tokunaga, J. Phys. Soc. Jpn. **84**, 073708 (2015).
[13] C. H. Li, Y. J. Long, L. X. Zhao, L. Shan, Z. A. Ren, J. Z. Zhao, H. M. Weng, X. Dai, Z. Fang, and C. Ren, Phys. Rev. B **95**, 125417 (2017).
[14] P. Di Pietro, M. Mitrano, S. Caramazza, F. Capitani, S. Lupi, P. Postorino, F. Ripanti, B. Joseph, N. Ehlen, and A. Grüneis, Phys. Rev. B **98**, 165111 (2018).
[15] P. L. Gong, B. Deng, L. F. Huang, L. Hu, W. C. Wang, D. Y. Liu, X. Q. Shi, Z. Zeng, and L. J. Zou, J. Phys. Chem. C **121**, 20931 (2017).
[16] T. Ando, J. Phys. Soc. Jpn. **74**, 777 (2005).
[17] T. Osada, J. Phys. Soc. Jpn. **77**, 084711 (2008).
[18] D. T. Son and B. Z. Spivak, Phys. Rev. B **88**, 104412 (2013).
[19] C. P. Slichter, *Principles of Magnetic Resonance*, 3rd ed. (Springer-Verlag, New York, 1989).
[20] S. Endo, Y. Akahama, S. Terada, and S. Narita, Jpn. J. Appl. Phys. **21**, L482 (1982).
[21] See Supplemental Material at http://link.aps.org/supplemental/10.1103/PhysRevLett.130.076401 for additional information on the stability of SMs to measure the long T_1 and the determination of T_1 from recovery curves, which includes Ref. [22].
[22] D. Ohki, M. Hirata, T. Tani, K. Kanoda, and A. Kobayashi, Phys. Rev. Res. **2**, 033479 (2020).
[23] F. Bridges and W. G. Clark, Phys. Rev. **182**, 463 (1969).
[24] T. Konoike, K. Uchida, and T. Osada, J. Phys. Soc. Jpn. **81**, 043601 (2012).
[25] L. Li, F. Yang, G. J. Ye, Z. Zhang, Z. Zhu, W. Lou, X. Zhou, L. Li, K. Watanabe, T. Taniguchi, K. Chang, Y. Wnag, X. H. Chen, and Y. Zhang, Nat. Nanotechnol. **11**, 593 (2016).
[26] When we take into account the Zeeman splitting of the Landau quantization, E should be replaced by E_+ and E_- on the right side of Eq. (2), where $E_\pm = E \pm g\mu_B B/2$, so that

$$D(E) = \frac{eB}{4\pi^2\hbar c v_F} \times \left(2 + 2\sum_{n=1}^{\lfloor E_+^2/2v_F^2 e\hbar B\rfloor} \frac{|E_+|}{\sqrt{E_+^2 - E_n^2}} + 2\sum_{n=1}^{\lfloor E_-^2/2v_F^2 e\hbar B\rfloor} \frac{|E_-|}{\sqrt{E_-^2 - E_n^2}}\right).$$

[27] P. E. Ashby and J. P. Carbotte, Eur. Phys. J. B **87**, 1 (2014).
[28] J. Klier, I. V. Gornyi, and A. D. Mirlin, Phys. Rev. B **92**, 205113 (2015).
[29] Y. Akahama, M. Miyakawa, T. Taniguchi, A. Sano Furukawa, S. Machida, and T. Hattori, J. Chem. Phys. **153**, 014704 (2020).
[30] For the present LDA calculation, we adopted $a = 3.3135$ Å, $b = 10.2440$ Å, and $c = 4.2744$ Å obtained at 1.55 GPa [29].
[31] T. Fujii, Y. Nakai, Y. Akahama, K. Ueda, and T. Mito, Phys. Rev. B **101**, 161408(R) (2020).
[32] Y. Nakai, Y. Koshita, T. Fujii, Y. Akahama, K. Ueda, and T. Mito (to be published).